NUMERICAL SIMULATION OF NAVIER-STOKES EQUATIONS FOR HELICOPTER ROTOR IN FORWARD FLIGHT USING MOVING CHIMERA GRIDS

Z. D. Qiao, A.M.Yang, B.Zhu
The Center for Aerodynamic Design and Research
Northwestern Polytechnical University,
Xian, 710072, China

Keywords: *Helicopter Rotor, Forward Flight, Full Implicit Dual Time Method, Navier-Stokes Equations, Unsteady Viscous Flow*

Abstract

At present dual time methods with explicit inner iteration scheme have been adopted by the most of unsteady flow simulations based on Euler equations or Navier-Stokes equations. A disadvantage of the methods is that the computation efficiency is not enough to calculate the complex unsteady flows. In this paper a full implicit dual time method with implicit pseudo-time scheme by using moving chimera grids is developed for computation of complex unsteady flows. In the method a high efficient implicit LU-SSOR method is adopted for the inner iteration computation.

The numerical tests of the unsteady flow simulation based on Navier-Stokes equations for forward flight of rotary wings show that the computation results is in agreement with experiment and the method is very efficient for computation of complex unsteady flows.

1 Introduction

Various methods have been developed for helicopter rotor problems based on potential, Euler and Navier-Stokes equations respectively. The classical lifting-line or lifting-surface theory based on potential equation has advantage of being a quick, simple method and works well if the nonlinear effects are negligible. And in this case theoretical vorticity cannot occur in a potential flow field except as discrete embedded filaments or sheets. The methods based on Euler equation provide proper modeling of vorticity transport, but the omission of viscosity means that there is still no built in mechanism for diffusion of the vortex wake. In addition, Euler equations are also inadequate when large scale separation or other significant viscous effects exist. Navier-Stokes Simulations for many complex aerodynamic problems have been made great progress, but their use in helicopter rotor analysis has been limited. Because the flow about helicopter rotor in forward flight is a kind of complex unsteady viscous flow, the numerical simulation based on Navier-Stokes equations are prohibitively expensive for use in practical engineering application. Typical flow solvers for unsteady flow computation employ dual time method. In this method Navier-Stokes equations are discretized with implicit method and then the discretized equation can be treated as a steady state problem to be solved explicitly by a pseudo-time. In order to achieve convergence within each physical time step, these dual time stepping schemes require a substantial number of pseudo-time steps. Another disadvantage of the dual time stepping method is that there are no available error estimates for time accuracy available, unless the inner iterations are fully converged.

In order to simulate the full unsteady viscous flows about helicopter rotors for engineering use, the efficiency of the underlying numerical algorithms needs to be improved. In this paper an improved dual time stepping method with implicit inner iteration scheme is developed. In the method a Newton-like inner iterations based on LU-SSOR Scheme are adopted.

The moving overset grid method[1] is employed to account the relative motion among the blades which are rotating, cyclic pitching and cyclic flapping. To build the connection among the overset grids quickly, a highly automatic and very efficient method based on Hole Map and Inverse Map is implemented.

2 Full Implicit Dual Time Method

By using finite volume method, in cell (*i,j,k*) Navier-Stokes equations can be discretized as following.

$$\frac{d\vec{w}_{i,j,k}}{dt} + \vec{R}_{i,j,k} = 0 \tag{1}$$

where

$$\vec{R}_{i,j,k} = \frac{1}{V_{i,j,k}}(\vec{E}_{i,j,k} + \vec{N}_{i,j,k} + \vec{D}_{i,j,k}) \tag{2}$$

and $\vec{E}_{i,j,k}$, $\vec{N}_{i,j,k}$ and $\vec{D}_{i,j,k}$ represent convective flux, physical viscous flux and artificial viscous flux respectively, $V_{i,j,k}$ is volume of cell (i ,j ,k).

Using backward difference scheme with the second order in Δt, we have

$$\frac{d}{dt}(\vec{W}^{n+1}_{i,j,k}) = \frac{3\vec{W}^{n+1}_{i,j,k} - 4\vec{W}^{n}_{i,j,k} + \vec{W}^{n-1}_{i,j,k}}{2\Delta t} \tag{3}$$

Let

$$\vec{R}^{*}_{i,j,k} = \frac{d}{dt}(\vec{W}^{n+1}_{i,j,k}) + \vec{R}^{n+1}_{i,j,k} \tag{4}$$

We can get

$$\frac{d\vec{W}^{*}}{d\tau} + \vec{R}^{*}(\vec{W}^{*}) = 0 \tag{5}$$

The equation (5) is a inner iteration scheme, τ is a fictitious time. Generally the equation (5) is solved by using explicit method, for example, Runge-Kutta method with second order in time. In the present paper we use following implicit scheme to solve the equation (5),

$$\frac{(\vec{W}^{*})^{m+1} - (\vec{W}^{*})^{m}}{\Delta\tau} + \frac{3(\vec{W}^{*})^{m+1} - 4\vec{W}^{n} + \vec{W}^{n-1}}{2\Delta t} + \vec{R}^{m+1}(\vec{W}^{*}) = 0 \tag{6}$$

In order to linearize the equation (6), we use the Taylor's expansion and obtain the following expression approximately

$$\vec{R}^{m+1} \approx \vec{R}^{m} + \left[\frac{\partial\vec{R}}{\partial\vec{W}^{*}}\right]^{m}\Delta\vec{W}^{*} \tag{7}$$

and m is a number for representation of the pseudo-time level, when $m \to \infty$, $(\vec{W}^{*})^{m+1} \to \vec{W}^{n+1}$, where

$\Delta\vec{W}^{*} = (\vec{W}^{*})^{m+1} - (\vec{W}^{*})^{m}$

Using equation (7) the equation (6) can be rewriten as

$$\frac{\Delta\vec{W}^{*}}{\Delta\tau} + \frac{3}{2\Delta t}\Delta\vec{W}^{*} + \left[\frac{\partial\vec{R}}{\partial\vec{\omega}^{*}}\right]^{m}\Delta\vec{W}^{*} = -\left[\frac{3\vec{W}^{*} - 4\vec{W}^{n} + \vec{W}^{n-1}}{2\Delta t} + \vec{R}^{m}(\vec{W}^{*})\right] \tag{8}$$

Because we only need to obtain the steady state solution of equation (8), we can get the following Newton inner iteration equation by letting $\Delta\tau \to \infty$.

$$\left\{\frac{3}{2\Delta t}I + \left[\frac{\partial\vec{R}}{\partial\vec{W}^{*}}\right]^{m}\right\}\Delta\vec{W}^{*} = -\left[\frac{3\vec{W}^{*} - 4\vec{W}^{n} + \vec{W}^{n-1}}{2\Delta t} + \vec{R}^{m}(\vec{W}^{*})\right] \tag{9}$$

In order to solve the equation (9), we use LU-SSOR implicit scheme, which does not need to solve inverse matrix.

3 Results

The full implicit dual time method has been applied to the numerical simulation of the flow about helicopter rotor in forward flight using Navier-Stokes equations with Baldwin-Lomax turbulence model. A model helicopter rotor was used for the computation, which was studied experimentally by caradonna [9] they tested a stiff, two-bladed untwisted rotor with constant chord and an NACA 0012 profile. The figure 1a shows the moving chimera grid system for hover flight. The figure 1b shows the moving chimera grid system for the computation in forward flight case. The grid system for forward flight consists of blade grids, background grids and the transition grids. The total number of grid points (including all two blades) is 2049792. The time step (Δt) taken in the calculation corresponds to an azimuth angle step of 0.03 degrees.

In the first test case advance ratio $\mu = 0.20$, tip Mach number $M_{tip} = 0.8$, pitch angle $\theta = 0°$, Renolds number $\mathrm{Re} = 2.89 \times 10^6$. The computation results are given in Fig.2. The computation results show good agreement with the experiment data.

In the second case, advance ratio $\mu = 0.15$, tip Mach number M_{tip}=0.671, the Reynolds number $\mathrm{Re} = 3.0 \times 10^6$, pitch angle $\theta(t) = 8° + 1.11° \cos\psi(t) - 3.23 \sin\psi(t)$, ψ is azimuth angle. Figure 3 shows profile pressure distributions of the rotor at radial location r/R=0.89 and the azimuth angle ψ=0°, 90°, 135°, 180°, 270°, 315° respectively. Figure 4 shows pressure contours on the upper surface of the rotor at ψ=135°, 180°. Figure 5 shows the thrust coefficient of the rotor as a function of azimuth ψ. From the Figure 5 it is can be seen that the history of thrust coefficient computation shows that the periodic solutions are obtained in third revolution of the rotor. Figures 6a-6b show vorticity contours of the rotor at ψ=90°, 180°.

References

[1] Yang, A.M. and Qiao, Z.D**.** *Numerical Simulation of Unsteady Flow Around a Helicopter Rotor in Forward Flight Using Moving Overset Grids.* ACTA AERODYNAMICA SINICA, pp.427-433,Vol.18, No.4, 2000

[2] Yang,S.C. and Qiao, Z.D. *Navier-Stokes Calculations of Transonic Viscous Flow over Finite Wings.* ACTA AERODYNAMICA SINICA, pp.243-249,Vol.18, No.2, 1998

[3] Yang, Y. and Qiao, Z.D. *Time Accurate 2D Navier-Stokes Calculations with a Dual-Time Stepping Method,* Chinese Journal of Aeronautics, PP.168-173, Vol.10, No.3,1997

[4] Yang, A.M. Qiao, Z.D. and Weng, P. F. *Numerical Simulation of the Viscous Flow past a Helicopter Rotor in Forward Flight Using Newton-Like Sub-Iterations.* ACTA AERODYNAMICA SINICA, PP.57-63, Vol.20,No.1,2002

[5] Hsu, J.M. and Jameson,A. *An Implicit- Explicit Hybrid Scheme for Calculating Complex Unsteady Flows.* AIAA paper 2002-0714,2002

[6] Yoon, S. and Jameson, A. *An LU-SSOR Scheme for the Euler and Navier-Stokes Equations.* AIAA paper 87-0600, 1987.

[7] Simpson, L.B. *Unsteady Three-Dimensional Thin-Layer Navier-Stokes Solutions on Dynamic Blocked Grids.* AFATL-TR-89-19,1989

[8] Jameson, A. *Time Dependent Calculations Using Multigrid with Applications to Unsteady Flows Past Airfoils and Wings,* AIAA paper 91-1596,1991.

[9] Caradonna, F.X. Laub, G.H., and Tung, C. *An Experimental Investigation of the parallel Blade-Vortex Interaction,* NASA TM-86005, 1984

[10] Webster, R.S., Chen, J.P. and Whitfield, D.L. *Numerical Simulation of a Helicopter Rotor in Hover and Forward Flight,* AIAA Paper 95-0193, 1995

[11] Ahmad, J. and Duque, E.P.N. *Helicopter Rotor Blade Computation in Unsteady Flows Using Moving Overset Grids.* Journal of Aircraft, PP.54-60, Vol.33, No.1, 1996

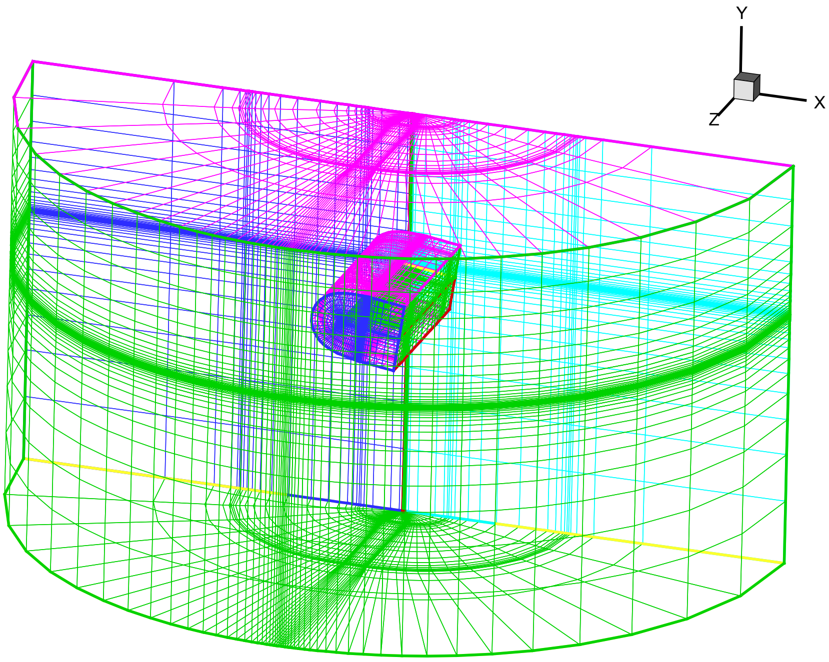

Fig.1a Moving chimera grid system for hover flight

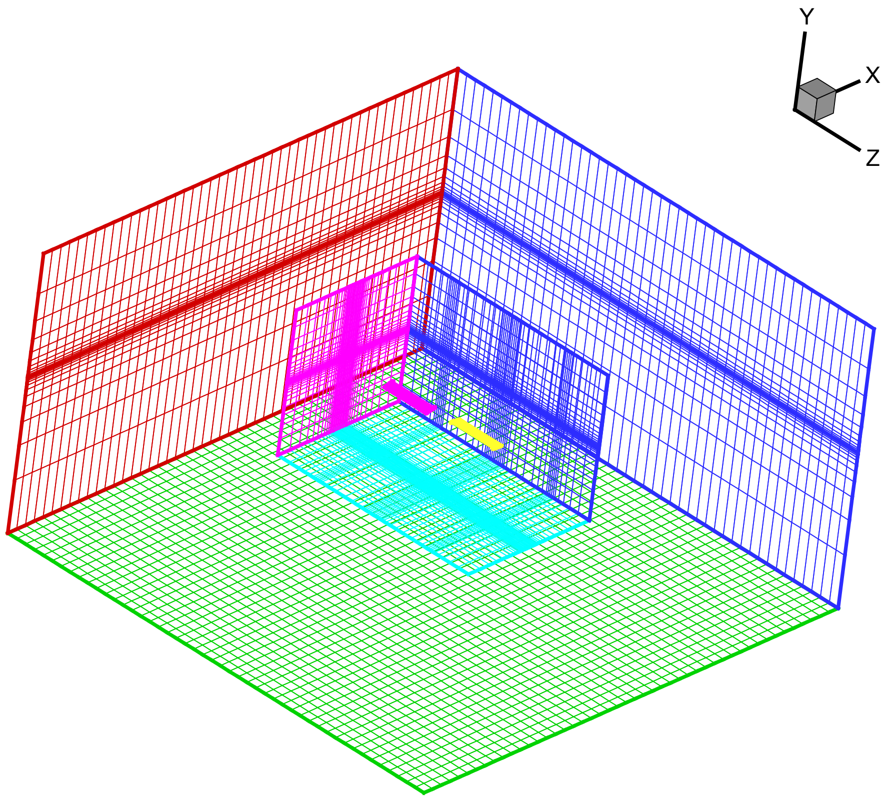

Fig.1b Moving chimera grid system for forward flight

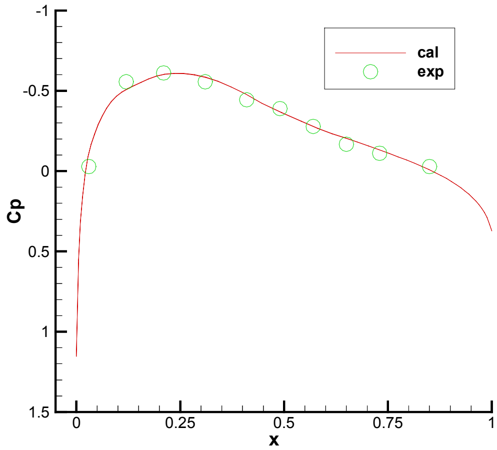

(a) $\psi = 30^{\circ}$

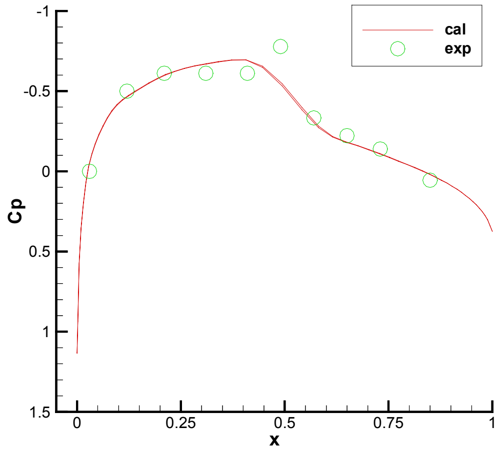

(b) $\psi = 60^{\circ}$

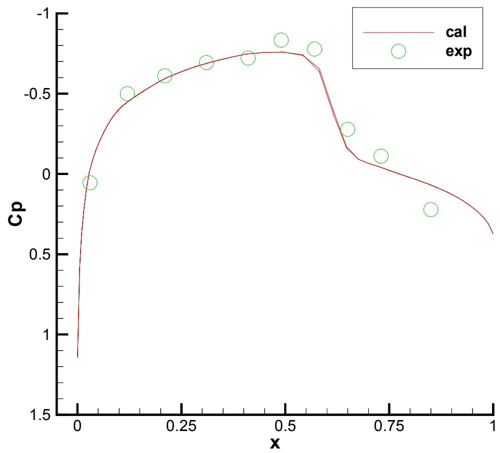

(c) $\psi = 90^{\circ}$

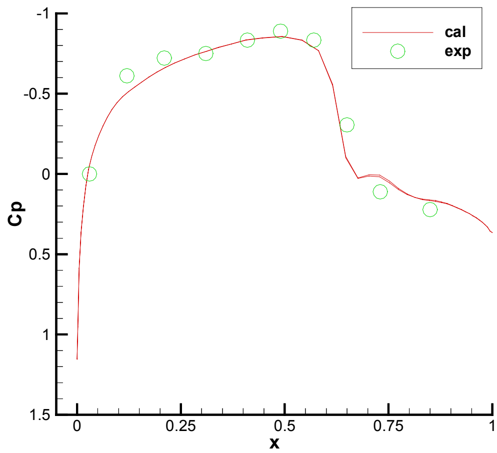

(d) $\psi = 120^{\circ}$

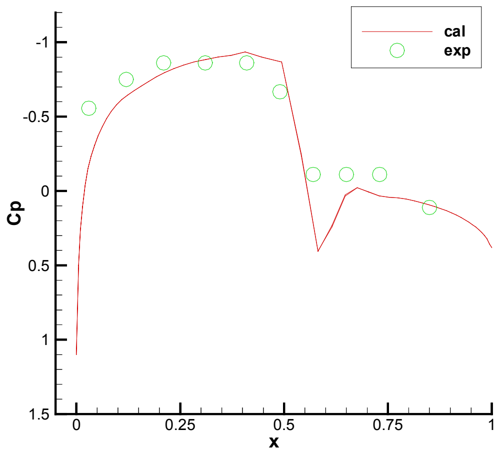

(e) $\psi = 150^{\circ}$

Fig.2 Pressure comparison between computation and experiment (first test case)

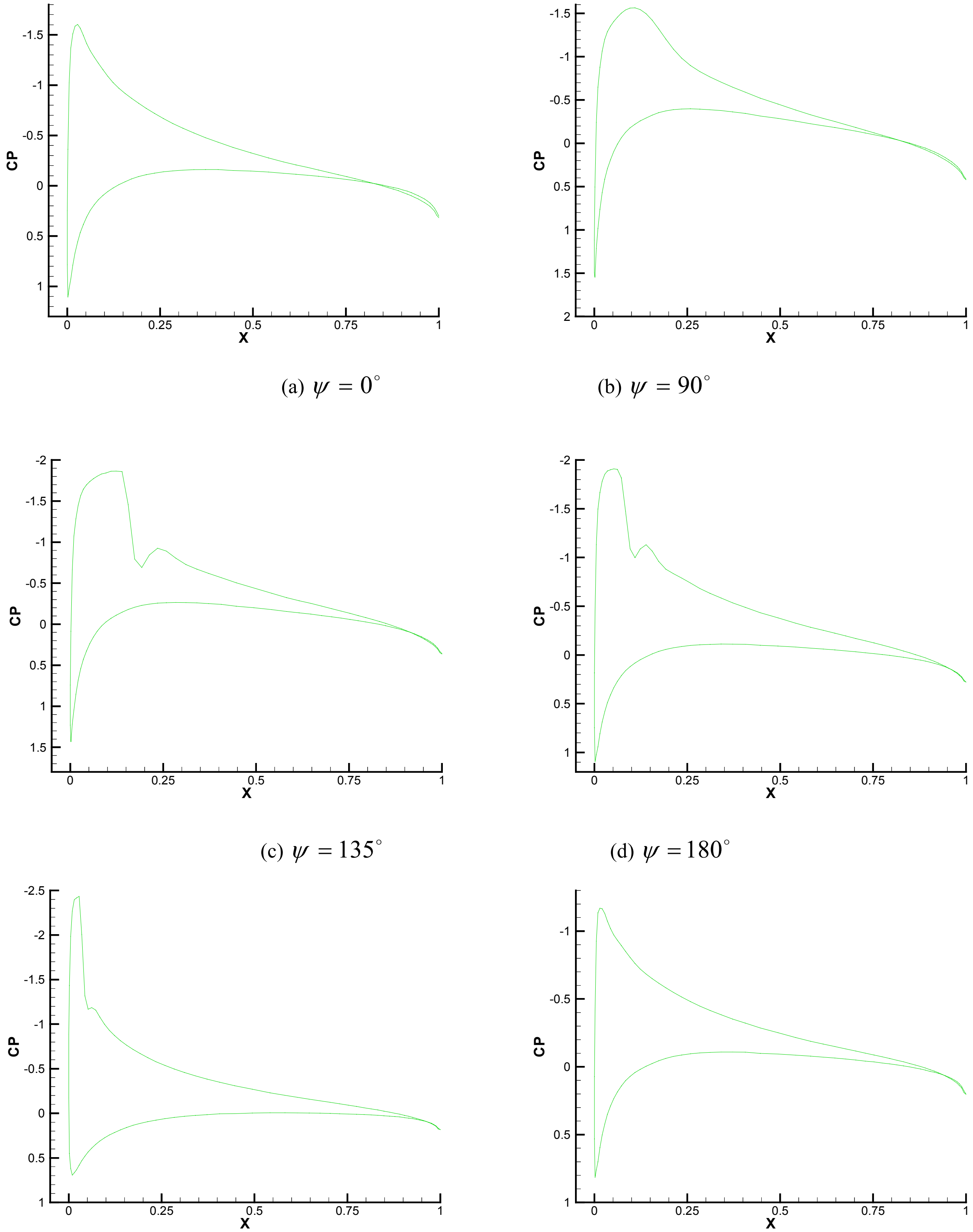

(a) $\psi = 0^{\circ}$ (b) $\psi = 90^{\circ}$

(c) $\psi = 135^{\circ}$ (d) $\psi = 180^{\circ}$

(e) $\psi = 270^{\circ}$ (f) $\psi = 315^{\circ}$

Fig.3 Pressure distributions of the helicopter rotor (second test case) at r/R=0.96

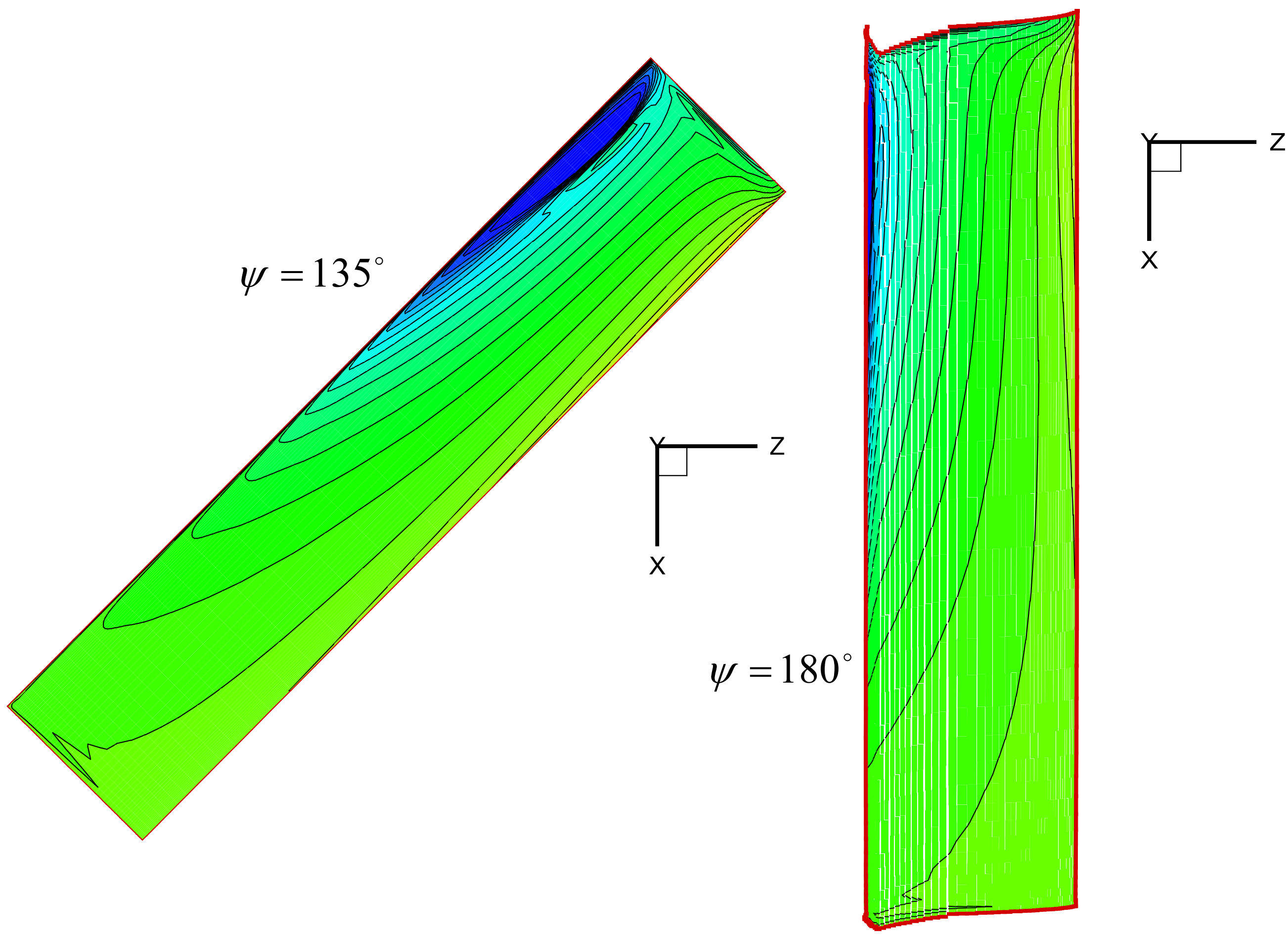

Fig.4 Pressure contours on the upper surface of the helicopter rotor (second test case)

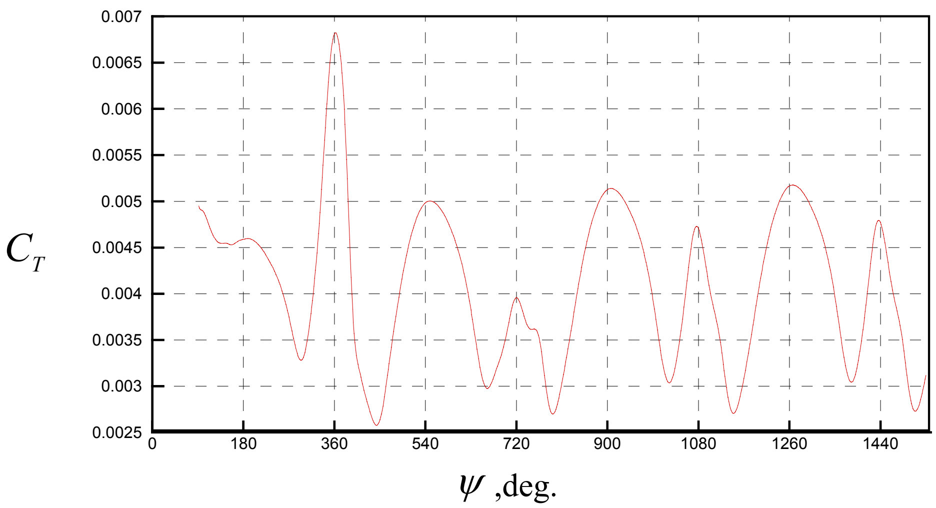

Fig.5 Thrust coefficient

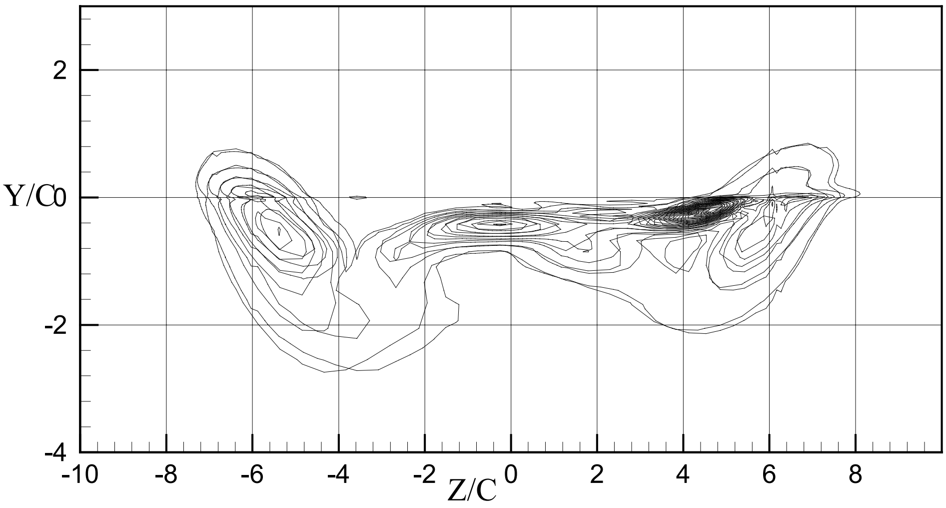

X/C = 4.5

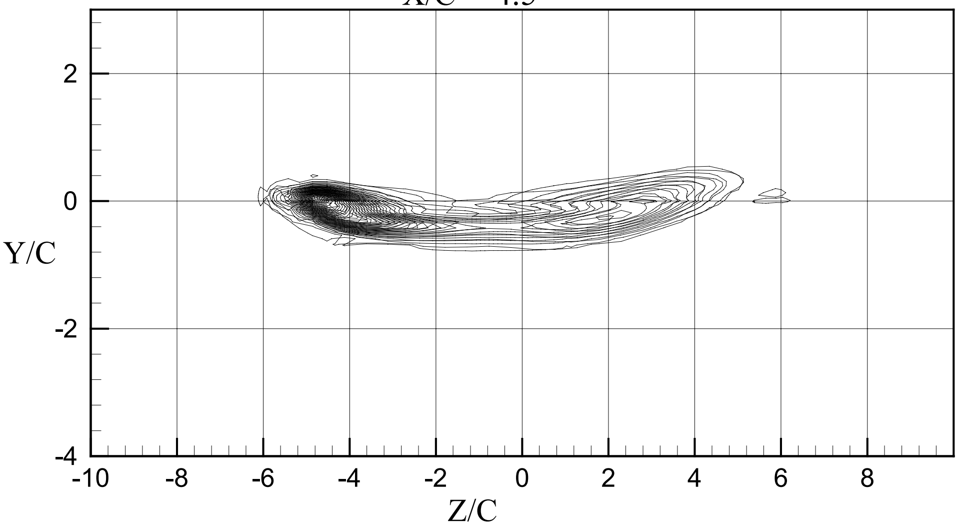

X/C = −4.5

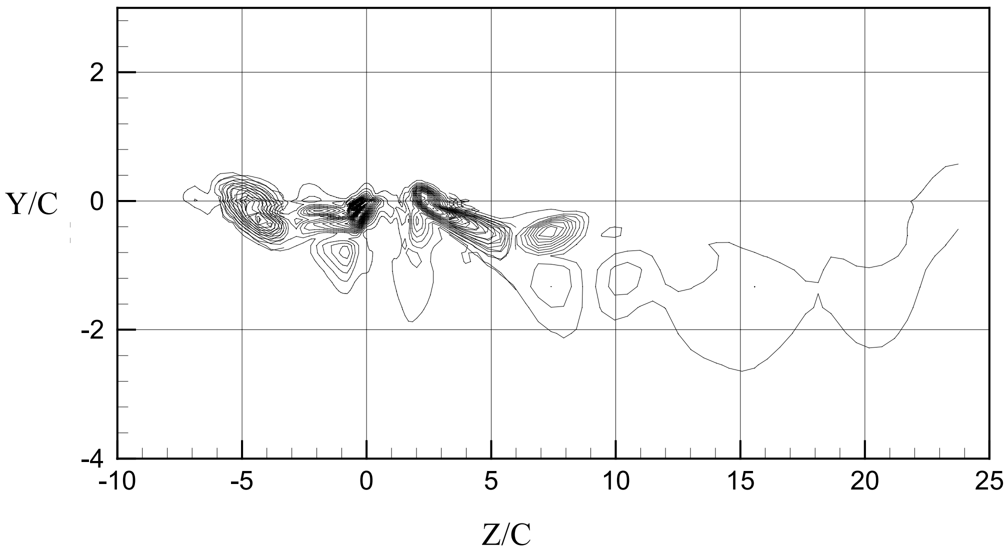

Z/C = 0

Fig. 6 a Vorticity contours of the helicopter rotor (the second test case) ($\psi = 90^{\circ}$)

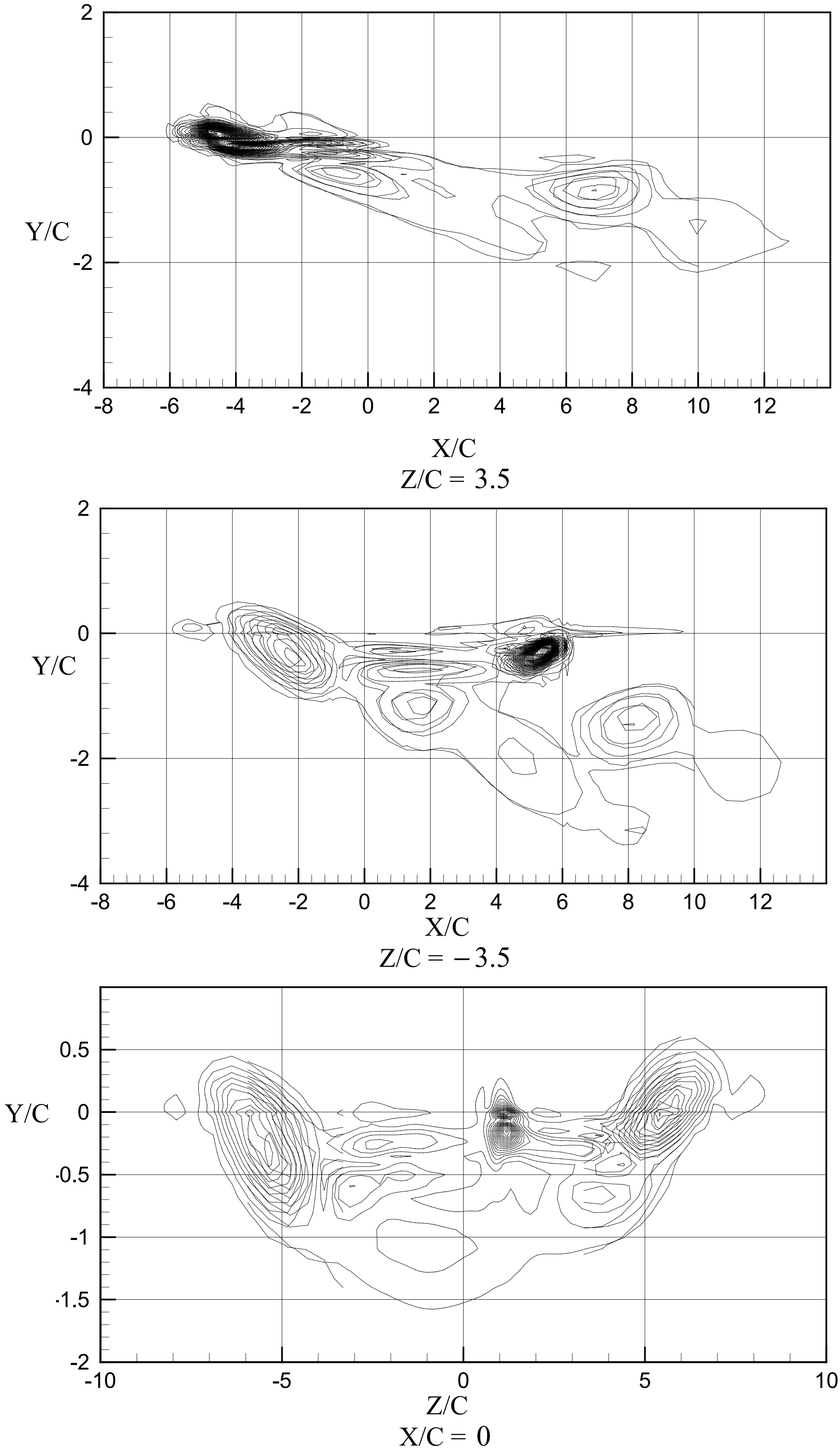

Fig. 6 b Vorticity contours of the helicopter rotor (the second test case) ($\psi = 180^\circ$)